The force acting on a superparamagnetic bead due to an applied magnetic field

Sergey S. Shevkoplyas,*[a] Adam C. Siegel,[a] Robert M. Westervelt,[bc] Mara G. Prentiss[c] and George M. Whitesides*[a]

Received 3rd April 2007, Accepted 25th June 2007
First published as an Advance Article on the web 25th July 2007
DOI: 10.1039/b705045c

This paper describes a model of the motion of superparamagnetic beads in a microfluidic channel under the influence of a weak magnetic field produced by an electric current passing through a coplanar metal wire. The model based on the conventional expression for the magnetic force experienced by a superparamagnetic bead (suspended in a biologically relevant medium) and the parameters provided by the manufacturer failed to match the experimental data. To fit the data to the model, it was necessary to modify the conventional expression for the force to account for the non-zero initial magnetization of the beads, and to use the initial magnetization and the magnetic susceptibility of the beads as adjustable parameters. The best-fit value of susceptibility deviated significantly from the value provided by the manufacturer, but was in good agreement with the value computed using the magnetization curves measured independently for the beads from the same vial as those used in the experiment. The results of this study will be useful to researchers who need an accurate prediction of the behavior of superparamagnetic beads in aqueous suspensions under the influence of weak magnetic fields. The derivation of the force on a magnetic bead due to a magnetic field also identifies the correct treatment to use for this interaction, and resolves discrepancies present throughout the literature.

Introduction

Superparamagnetic beads are important in a multitude of biological and biomedical applications,[1–4] including manipulation[5] and separation[6–8] of cells, isolation of specific cells in immunomagnetic assays,[1,9] separations of proteins,[10] and application of mechanical forces to cells.[11] Suspensions of superparamagnetic beads in biocompatible aqueous buffers are often used in conjunction with microfluidic and other types of microfabricated devices.[2,3] Macroscopic permanent magnets and electromagnets can produce magnetic fields sufficiently strong (>0.5 T) to saturate the magnetization of superparamagnetic beads; under these circumstances, the beads behave simply as permanent magnets. Microfabricated electromagnets produce magnetic fields too weak (0–10 mT) to saturate the magnetization of the beads (see Siegel *et al.*[12] and references therein). In this range of magnetic field strengths, the magnetization of the beads is a complex, multi-valued function of the applied magnetic field (see, for example, Fig. 1).

Eqn (1) is the relationship most often cited in the literature[2] for the force acting on a magnetic particle inside a magnetic field; here V is the volume of the particle (m^3), $\Delta\chi$ is the difference in magnetic susceptibilities between the particle and the surrounding medium (dimensionless), $\mu_0 = 4\pi \times 10^{-7}$ (T m A^{-1}) is the permeability of vacuum, and $\vec{B}$ is the applied magnetic field (T).

$$\vec{F} = \frac{V\Delta\chi}{\mu_0}\left(\vec{B}\cdot\nabla\right)\vec{B} \quad (1)$$

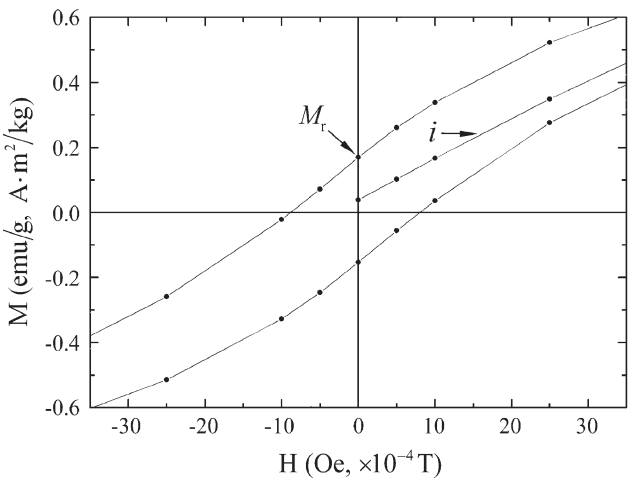

Fig. 1 Magnetic response of COMPEL™ superparamagnetic beads (nominal diameter 6 μm) in weak fields ranging from −3.5 to 3.5 mT measured with a SQUID magnetometer at room temperature (300 K) by the manufacturer (Bangs Laboratories, Inc.). The magnetization of the beads saturates at 2.95 (A m^2 kg^{-1}) in fields stronger than ~0.5 T (not shown). Following saturation, the beads possess remnant magnetization M_r = 0.17 (A m^2 kg^{-1}) at zero field. The magnetic susceptibility of the beads, χ_{bead}= (0.170 ± 0.007), is calculated from the slope of a line fitted to the initial (*i*) part of the magnetization curve (0–2.5 mT); the spread represents the 95% confidence interval.

[a]*Department of Chemistry and Chemical Biology, Harvard University, 12 Oxford St., Cambridge, MA, 02138, USA. E-mail: gwhitesides@gmwgroup.harvard.edu; sshevkoplyas@gmwgroup.harvard.edu*
[b]*School of Engineering and Applied Physics, Harvard University, 29 Oxford St., Cambridge, MA, 02138, USA*
[c]*Department of Physics, Harvard University, 17 Oxford St., Cambridge, MA, 02138, USA*

Eqn (1) often appears in the literature without derivation or reference to a derivation.[2,13–18] The absence of an appropriate derivation makes it difficult to decide whether and how this formula should be used in a particular experiment.

This paper describes the correct way to compute the force experienced by a superparamagnetic bead (suspended in a biologically relevant medium) in an applied magnetic field that is not strong enough to saturate the magnetization of the bead (eqn (2)). In this equation, ρ is the density of the bead (kg m^{-3}), $\vec{M}_0$ is the initial magnetization of the bead (A m^2 kg^{-1}), and χ_{bead} is the initial magnetic susceptibility of the bead (dimensionless) obtained from the magnetization curve (Fig. 1) (we neglect the magnetic susceptibility of the suspending medium).

$$\vec{F} = \rho V \nabla\left(\vec{M}_0 \cdot \vec{B}\right) + \frac{V\chi_{\text{bead}}}{\mu_0}\left(\vec{B}\cdot\nabla\right)\vec{B} \qquad (2)$$

We use the two expressions for the force to model the motion of superparamagnetic beads in a microfluidic channel under the influence of a weak magnetic field produced by a coplanar electromagnet.[12] We demonstrate that a model based on the conventional expression (given by eqn (1)) and the value of the magnetic susceptibility of the beads obtained from the magnetization curve provided by the manufacturer does not match the experimental data. Using the initial magnetization and the susceptibility of the beads as adjustable parameters, we show that the model based on eqn (2) agrees well with the data. We find that the best-fit value of the magnetic susceptibility of the beads is nearly two times higher than the value provided by the manufacturer, but is in good agreement with the result of our own measurement of the magnetic response of the beads performed on a sample of the beads from the same vial as those used in the experiment.

Computation of the force acting on a superparamagnetic bead

Superparamagnetic beads as ideal magnetic dipoles

The internal structure of superparamagnetic beads can be very complex. Depending on the manufacturing procedure, each bead may consist of an iron oxide (magnetite, Fe_3O_4) particle with a functionalized coating,[19] a sphere of polymer matrix impregnated with iron oxide nanoparticles,[20,21] or a polymer sphere coated with iron oxide.[22] Because of this complexity, derivation of the magnetic moment of a bead ($\vec{m}_{\text{bead}}$), and prediction of the dependence of the magnetic moment on the applied magnetic field, from the bulk magnetic properties of the constituent materials can both be difficult or impossible. Fortunately, manufacturers of superparamagnetic beads measure the dependence of the average mass magnetization of the beads M ((emu g^{-1}) CGS, (A m^2 kg^{-1}) SI units) on the applied magnetic field, and generate empirical, so-called magnetization curves; Fig. 1 shows an example of such a curve for a sample of 6 μm beads (COMPEL, Bangs Laboratories, Inc.). In this figure, the applied magnetic field is denoted H and is shown in CGS units of Oersted (Oe) in accordance with the notation accepted in technical literature. In eqn (1) and (2), the applied magnetic field is denoted $\vec{B} \equiv \mu_0\vec{H}$ and is expressed in the SI units of Tesla (T).

In weak magnetic fields ($B \equiv \mu_0 H \leqslant 3$ mT as in Fig. 1), the magnetization of a superparamagnetic bead $\vec{M}$ depends approximately linearly on the applied magnetic field (eqn (3)), where $\vec{M}_0$ is the initial magnetization (A m^2 kg^{-1}) and χ_{bead} is the initial magnetic susceptibility of the bead (dimensionless).

$$\vec{M} = \vec{M}_0 + \frac{\chi_{\text{bead}}}{\rho}\vec{H} = \vec{M}_0 + \frac{\chi_{\text{bead}}}{\rho}\frac{\vec{B}}{\mu_0} \qquad (3)$$

The initial magnetic susceptibility χ_{bead} is defined as the slope of the initial (starting from the fully relaxed state) part of the magnetization curve (i in Fig. 1) and is given by eqn (4) (where the conversion of units is required if ΔM and ΔH are expressed in the units of CGS). The susceptibility χ_{bead} calculated this way is an average property—the magnetic susceptibility of individual beads may vary significantly even within the same lot.[23] The empirical dependence of the effective magnetic moment of an average individual bead $\vec{m}_{\text{bead}}$ (A m^2) on the applied magnetic field is then given by eqn (5). Eqn (5) should hold as long as the applied magnetic field in an experiment remains within the same range and along the same path around the hysteresis loop as that used in measuring the magnetization curve.

$$\chi_{\text{bead}} \equiv \rho\frac{\Delta M}{\Delta H}\left[\left(\text{kg m}^{-3}\right)\left(\text{emu g}^{-1}\right)\text{Oe}^{-1}\right] = \frac{4\pi}{10^3}\rho\frac{\Delta M}{\Delta H} \qquad (4)$$

$$\vec{m}_{\text{bead}} = \rho V\vec{M} = \rho V\left(\vec{M}_0 + \vec{M}\left(\vec{B}\right)\right) = \rho V\left(\vec{M}_0 + \frac{\chi_{\text{bead}}}{\rho\mu_0}\vec{B}\right) \qquad (5)$$

We note that because the bead can rotate freely in suspension, $\vec{M}_0$ is always parallel to the applied field $\vec{H}$ so long as the bead is spherical and its magnetic response is isotropic. We also emphasize that the value of the initial magnetization of the bead $\vec{M}_0$ (*i.e.*, the magnetization of the bead in the absence of the applied magnetic field) depends on the history of prior magnetization of the bead. In general, the value of $\vec{M}_0$ for a specific bead may be anything from zero to M_r (remnant magnetization, see Fig. 1). The fact that the initial part of the magnetization curve shown in Fig. 1 does not start from zero (seemingly suggesting a non-zero magnetization of the sample at zero applied field) is misleading. A sample of the beads for a SQUID (superconducting quantum interference device) magnetometer is usually prepared in the form of dry powder containing tens of millions of beads in random orientations—the magnetization of the sample at zero applied field must be zero even when the initial magnetizations, $\vec{M}_0$, of individual beads are not. The apparent non-zero initial magnetization shown in Fig. 1 is likely due to a slightly positive remnant field trapped in the superconducting magnet of the SQUID magnetometer.[24–26]

In the derivation of eqn (5) for the magnetic moment of the bead, we have neglected the magnetic properties of the medium in which the bead is suspended. How valid is this assumption? The magnetic susceptibility of water is approximately -9×10^{-6}. The larger lanthanide salts possess some of the highest molar magnetic susceptibilities known;[27] for example, Winkleman *et al.*[28] showed that the magnetic susceptibility of aqueous solutions of $GdCl_3$ at concentrations compatible with living mammalian cells (40 mM) is 1.4×10^{-5}. Because these values are at least four orders of magnitude smaller than

the susceptibility of the beads (χ_{bead} = (0.170 ± 0.007), Fig. 1), we can safely neglect the effect of the magnetic properties of suspending medium for a majority of biological and biomedical applications.[29]

The manufacturer obtains magnetization curves by measuring the change in magnetization of a sample of the beads in response to a specified range of applied magnetic fields (Fig. 1). From these curves we obtain the effective dependence of $\vec{M}$, *i.e.* the magnetic moment of the beads per unit mass, on the applied field $\vec{H}$ (or $\vec{B} \equiv \mu_0 \vec{H}$ as in eqn (1) and (2)); we do not consider the total macroscopic field inside the bead $\vec{B}_{total} = \mu_0 \left(\vec{H} + \rho \vec{M} \right)$, as is commonly done in the textbooks.[30,31] Practically, $\vec{M}$ *vs.* $\vec{H}$ is exactly what we need—in an experiment, we are likely to know the applied field, $\vec{H}$, which we would generate by passing electric current through a conductor of known geometry, and have no way to measure the total field inside the bead.[31]

Because we now know explicitly how the magnetic moment of a bead depends on the applied magnetic field (eqn (5)), we can neglect the details of the complicated, heterogeneous structure of the superparamagnetic bead, and treat the bead as an ideal (point) magnetic dipole with the magnetic moment equal to the effective magnetic moment of the bead $\vec{m}_{bead}$. We note that a rigorous derivation of the functional dependence of $\vec{m}_{bead}$ on the applied field would be difficult: one would have to consider the magnetic properties of the heterogeneous mixture of magnetic and non-magnetic materials comprising the bead (which may be unknown) and the shape of the bead, and solve the boundary value problem for the magnetic field vectors $\vec{H}$ and $\vec{B}_{total}$ in the specific geometry of an experiment.[32] We do not have to perform this intractably complex calculation because we know how the actual beads respond to the applied field exactly, thanks to the empirical magnetization curve.

Calculation of the force

The magnetic force acting on a magnetic dipole, $\vec{m}$, in an applied magnetic field, $\vec{B}$, is generally given by eqn (6).[30–32] By substituting the empirical expression for the magnetic moment $\vec{m}_{bead}$ of the superparamagnetic bead (eqn (5)) into eqn (6), we obtain eqn (7) for the force acting on the bead.

$$\vec{F} = (\vec{m} \cdot \nabla) \vec{B} \tag{6}$$

$$\vec{F} = (\vec{m}_{bead} \cdot \nabla) \vec{B} = \rho V \left(\vec{M}_0 \cdot \nabla \right) \vec{B} + \frac{V \chi_{bead}}{\mu_0} \left(\vec{B} \cdot \nabla \right) \vec{B} \tag{7}$$

If we neglect the effect of the magnetic properties of the suspending medium and use χ_{bead} obtained from the magnetization curve (Fig. 1) as the magnetic susceptibility of the bead, the conventional formula (eqn (1)) for the force acting on a superparamagnetic bead in magnetic field becomes eqn (8). (Note that because the conventional formula for the force (eqn (1)) does not account for the demagnetization field due to the shape of the particle,[32] we must use χ_{bead}, not the magnetic susceptibility of the material of the beads.)

$$\vec{F} = \frac{V \chi_{bead}}{\mu_0} \left(\vec{B} \cdot \nabla \right) \vec{B} \tag{8}$$

Clearly, the conventional expression for the force (eqn (8)) does not account for the initial magnetization of superparamagnetic beads, $\vec{M}_0$. The magnitude of the initial magnetization (however small it may be in absolute terms) can be comparable to the magnetization induced by a weak applied magnetic field (see Fig. 1). It should, therefore, be taken into account to describe the behavior of the beads realistically.

Model of an experiment

Description of the experiment

To test the accuracy of eqn (1) and (2), we used both expressions to model the motion of superparamagnetic beads in a microfluidic channel under the influence of a weak magnetic field produced by an electric current passing through a coplanar metal wire[12] (Fig. 2). The coplanar fabrication of the microfluidic channel and the metal wires embedded in poly(dimethylsiloxane) (PDMS), as well as the particulars of the experiment, have been described in detail elsewhere.[12] We loaded a suspension of superparamagnetic beads in phosphate-buffered saline (PBS) buffer into the middle microchannel using a syringe pump. When we stopped the flow, we observed that the beads were distributed approximately uniformly across the width of the channel (Fig. 2c). We passed electrical current, I (A), through one of the co-fabricated electromagnets, adjacent to the microfluidic channel, and measured the time (the capture time, t_{cap} (s)) it took for approximately 90% of the beads to reach the sidewall of the microfluidic channel closest to the active electromagnet (Fig. 2d). We performed this experiment several times by turning on/off left and right electromagnets sequentially to obtain multiple data (t_{cap}) for each value of the current.

Simplifications of the model

To model this experiment, we approximate the geometry of the real problem (Fig. 2) by a simplified version shown in Fig. 3, in which we represent the coplanar electromagnet by an infinitely long, cylindrical, conductive wire carrying electrical current.

The electric current I (A) passing through an infinitely long, cylindrical wire generates a magnetic field. Outside of the wire, at a distance r (m) from its center, the magnitude of the magnetic field B is given by eqn (9), and the direction of the magnetic field vector $\vec{B}$ is determined by the right-hand rule (Fig. 3).[33]

$$B = \frac{\mu_0 I}{2 \pi r} \tag{9}$$

In the model, we neglect inertia and the effect of the walls of the channel on the viscous drag experienced by a moving bead. In addition, we neglect the magnetic properties of the suspending medium, and assume that the initial magnetization of the bead $\vec{M}_0$ does not change during the course of the experiment. Finally, we assume that the beads are distributed *uniformly* across the width of the microfluidic channel in the beginning of the experiment. For a *uniform* distribution of the beads, measuring t_{cap} is equivalent to measuring the time required for a single bead to move from its initial position located 90% of the channel width away from the sidewall closest to the active electromagnet, a = 104 (μm), to its final position in contact with said sidewall, b = 73 (μm) (note that all distances are calculated

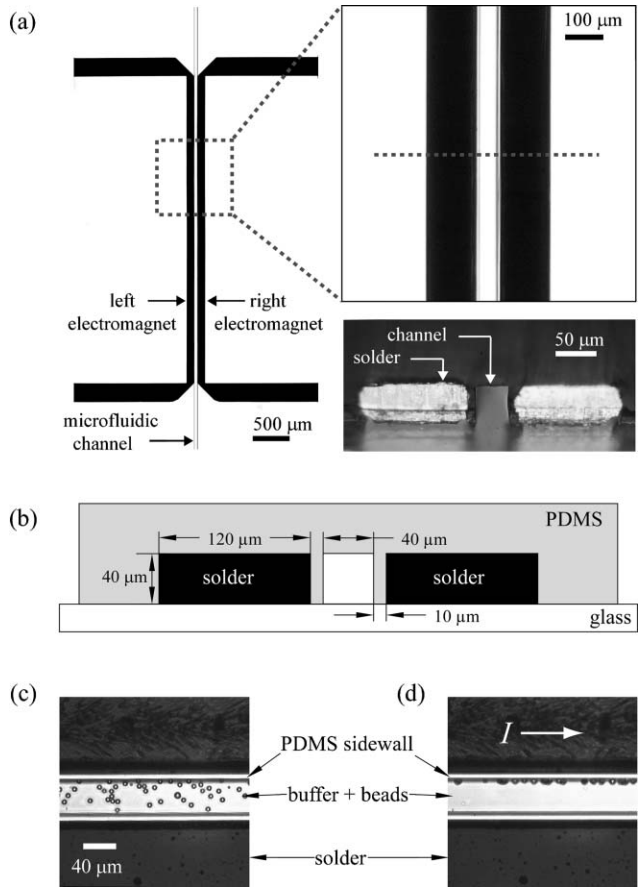

Fig. 2 (a) Photographs of the device, comprising two metal (low melting-point solder) wires co-fabricated astride a microfluidic channel (all in a microsystem fabricated in PDMS), as viewed from above at low magnification (left), high magnification (upper right) and in cross-section (lower right). The cross-section was obtained by sectioning the device with a razor blade along the dashed line in the upper right image; the dark line in the left electromagnet is the result of imperfect sectioning; the light areas at the bottom of the image are reflections of the metal in the glass support. In the photograph at low magnification, lines were drawn to outline the location of the microfluidic channel. (b) A schematic diagram of the cross-section of the device (lower right in panel (a)) showing the dimensions of key components of the device. (c) The microfluidic channel is filled with a suspension of superparamagnetic beads in a buffer; the beads are distributed uniformly across the channel. (d) Electrical current I passing through the top solder wire (electromagnet) produces magnetic field within the channel that magnetizes and attracts the beads towards the electromagnet. Panels (a), (c) and (d) are reproduced in part from Siegel *et al.*[12] with permission.

from the center of the active electromagnet and that the bead can not approach the wall closer than its radius) (Fig. 2b, 3).

The balance of forces

Two forces act on a superparamagnetic bead in the microchannel—the magnetic force, $\vec{F}_\mathrm{m}$, due to the gradient of the applied magnetic field, $\vec{B}$, produced by the electromagnet, and the Stokes force, $\vec{F}_\mathrm{s}$, due to the viscous drag exerted by the suspending medium on a moving bead (eqn (10)) (here $\vec{a}$ is the acceleration of the bead). The Stokes force is given by eqn (11), where η

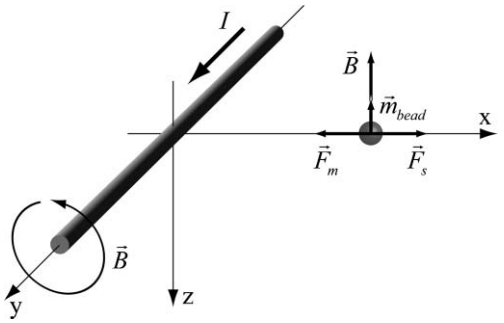

Fig. 3 An idealized representation of the superparamagnetic bead in the microfluidic channel with an adjacent metal wire (electromagnet). The electromagnet is represented by an infinitely long, cylindrical wire carrying electrical current.

(kg m^{-1} s^{-1}) is the dynamic viscosity of the suspending medium, $\vec{\mathrm{v}}$ is the velocity of the superparamagnetic bead (m s^{-1}), and R is the radius of the bead (m).[34]

$$\rho V\vec{a} = \vec{F}_\mathrm{m} + \vec{F}_\mathrm{s} \tag{10}$$

$$\vec{F}_\mathrm{s} = -6\pi\eta R\vec{\mathrm{v}} \tag{11}$$

Model based on eqn (1)

Using the expression for the magnetic field (eqn (9)) and some basic geometrical considerations (Fig. 3), we find that the only non-zero component of the magnetic force vector given by the conventional formula (eqn (8)) is the x component, given by eqn (12) (for details of the derivation please see the Appendix). We neglect the inertia of the superparamagnetic bead in eqn (10) for the balance of forces and, by substituting the magnetic force (eqn (12)) and the force of viscous drag (eqn (11)), we obtain eqn (13). We solve the differential eqn (13) in a closed form to find t_cap—the time it takes the average bead to move from its initial position, a, to its final position, b, near the sidewall of the channel closest to the electromagnet (eqn (14)).

$$F_\mathrm{m} = -\frac{\chi_\mathrm{bead} R^3 \mu_0 I^2}{3\pi x^3} \tag{12}$$

$$\frac{\mathrm{d}x}{\mathrm{d}t} = \beta x^{-3}, \text{ where } \beta = -\frac{\chi_\mathrm{bead} R^2 \mu_0 I^2}{18\pi^2\eta} \tag{13}$$

$$t_\mathrm{cap} = \frac{1}{4\beta}\left(b^4 - a^4\right) \tag{14}$$

Model based on eqn (2)

Using the same argument as for the model based on the conventional formula for the force, we obtain the following expression (eqn (15)) for the x component of the magnetic force vector given by eqn (7) (see Appendix). We again neglect inertia in the balance of forces (eqn (10)) and substitute eqn (15) for the magnetic force and eqn (11) for the force of

viscous drag into the balance to obtain eqn (16). Finally, we solve the differential eqn (16) in a closed form to find the capture time t_{cap}, which is given by eqn (17).

$$F_m = -\frac{2\rho M_0 R^3 \mu_0 I}{3x^2} - \frac{\chi_{bead} R^3 \mu_0 I^2}{3\pi x^3} \quad (15)$$

$$\frac{dx}{dt} = \alpha x^{-2} + \beta x^{-3}, \text{ where } \alpha = -\frac{\rho M_0 R^2 \mu_0 I}{9\pi\eta}$$

$$\text{and } \beta = -\frac{\chi_{bead} R^2 \mu_0 I^2}{18\pi^2 \eta} \quad (16)$$

$$t_{cap} = \frac{1}{3\alpha}(b^3 - a^3) - \frac{\beta}{2\alpha^2}(b^2 - a^2) + \frac{\beta^2}{\alpha^3}(b-a) - \frac{\beta^3}{\alpha^4}\ln\left(\frac{\alpha b + \beta}{\alpha a + \beta}\right) \quad (17)$$

Comparison of the two models with the experimental data

According to the certificate of analysis provided by the manufacturer, the diameter of the beads is $2R = (5.91 \pm 0.16)$ (μm) and the density of the beads is $\rho = 1089$ (kg m^{-3}). The dynamic viscosity of the suspending medium (PBS) is $\eta = 10^{-3}$ (kg m^{-1} s^{-1}). We used the room temperature (300 K) magnetization curve (Fig. 1) provided by the manufacturer (Bangs Laboratories, Inc.) to calculate the magnetic susceptibility of the beads χ_{bead}. To estimate the slope of the initial part (*i* in Fig. 1) of the magnetization curve, we fitted the points corresponding to the applied fields from 0 to 2.5 (mT) with a line and found, after the appropriate conversion of units (eqn (4)), that $\chi_{bead} = (0.170 \pm 0.007)$ (the spread in the value of the magnetic susceptibility represents the 95% confidence interval).

We used these parameters to evaluate t_{cap} as predicted by the model (eqn (14)) based on the conventional expression for the magnetic force acting on a superparamagnetic bead (eqn (1) or (8))—the capture times predicted by the model fail to match the experimental data (Fig. 4). The model (eqn (14)) overestimates the capture time by at least a factor of two—the model predicts that the beads should move more slowly than they actually do.

We treated the initial magnetization of the bead, M_0, and the susceptibility, χ_{bead}, as parameters and fitted the model (eqn (17)) based on the modified expression for the force (eqn (2) or (7)) to the experimental data, using the weighted linear least squares method (data with larger variances were assigned less weight). The best (in the weighted linear least squares sense) estimates for the initial magnetization of the beads and the susceptibility were $M_0 = 0.05$ (A m^2 kg^{-1}) and $\chi_{fit} = 0.36$ (Fig. 4, solid line, $R^2 = 0.9923$). The contribution from the non-zero initial magnetization is especially evident for small currents ($I < 0.2$ A), where the best-fit model deviates from a straight line to match the data (compare the shapes of the solid and the dashed line in Fig. 4). Expectedly, the estimated value of the initial magnetization of the beads M_0 is smaller than $M_r = 0.17$ (A m^2 kg^{-1})—the maximum possible value of the initial magnetization according to the magnetization curve (Fig. 1). The best-fit value of susceptibility ($\chi_{fit} = 0.36$) is, however, about two times higher than the value of susceptibility $\chi_{bead} = (0.170 \pm 0.007)$ calculated from the initial part of the magnetization curve provided by the manufacturer (Fig. 1).

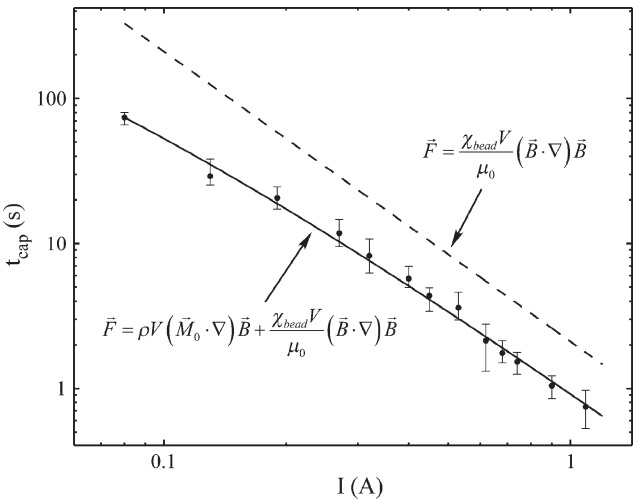

Fig. 4 A comparison of the experimental data (from Siegel *et al.*[12]) with the predictions of the model based on different versions of the formula for the magnetic force acting on the superparamagnetic bead. The error bars represent the range of the measured values. The dashed line corresponds to the model given by eqn (14) based on the conventional expression for the force; $\chi_{bead} = 0.17$ as provided by the manufacturer. The solid line is the best fit ($R^2 = 0.9923$) of the model given by eqn (17) based on the modified expression for the magnetic force ($M_0 = 0.05$ (A m^2 kg^{-1}), $\chi_{bead} = \chi_{fit} = 0.36$) to the experimental data.

To obtain an independent (from the manufacturer) estimate of the magnetic properties of the beads, we used a SQUID magnetometer (MPMS XL-7, Quantum Design) for measuring the magnetic response of a sample of the superparamagnetic beads from the same vial as the beads we used in the experiment (Fig. 5). We calculated the magnetic susceptibility of the beads $\chi_{bead} = (0.33 \pm 0.06)$ by fitting a line to the points of the initial part (*i* in Fig. 5) of the magnetization curve corresponding to the applied magnetic fields ranging from 0 to 2.5 mT. This value, $\chi_{bead} = (0.33 \pm 0.06)$, is in good agreement with the estimate of the best-fit value of magnetic susceptibility provided by the model ($\chi_{fit} = 0.36$). Similarly to the value of susceptibility, the saturation magnetization (4.13 A m^2 kg^{-1}) and the remnant magnetization ($M_r = 0.28$ (A m^2 kg^{-1})) of the beads are higher than the saturation magnetization (2.95 A m^2 kg^{-1}) and the remnant magnetization ($M_r = 0.17$ (A m^2 kg^{-1})) reported by the manufacturer.

One possible explanation of this discrepancy is the variability of the manufacturing process. The magnetization curves (such as the one shown in Fig. 1 or Fig. 5) are not routinely measured for each lot of the superparamagnetic beads produced and sold by the manufacturer, partially because the originally intended application for these beads (separation of cells) does not require precise knowledge of the magnetic properties of the beads in *weak* magnetic fields. For cell separation, the variability of the susceptibility of the beads between different lots is not important, because the magnetic separations of cells are usually carried out with the use of strong permanent magnets that saturate the magnetization of the beads. In this context, the possibility that the beads in some lots are "*more magnetic*" than those in others is only an advantage.

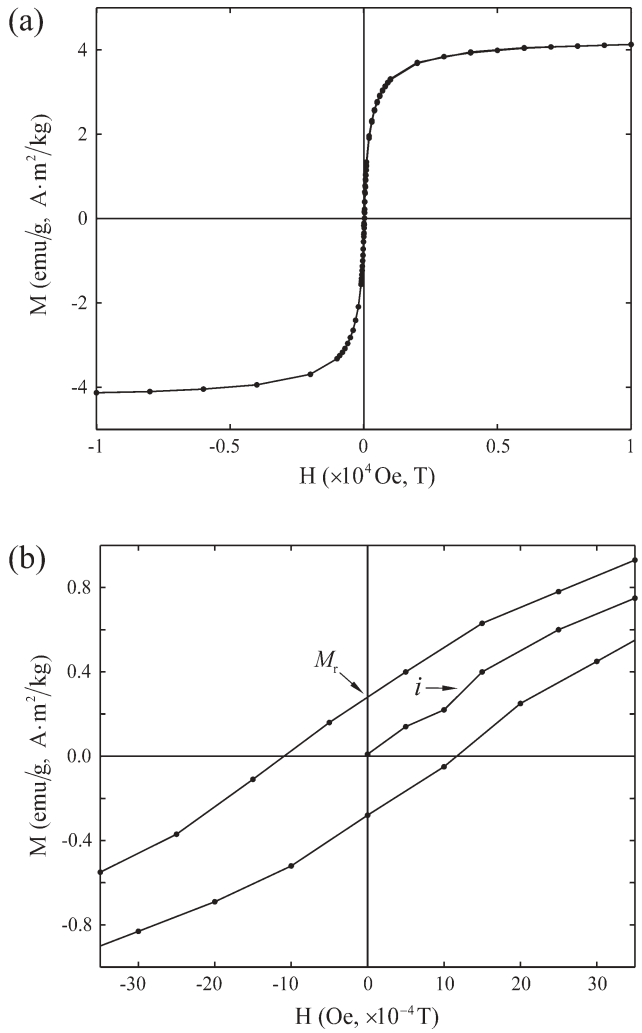

Fig. 5 Magnetization curve for a sample of superparamagnetic beads from the same vial as those used in the experiment (actual diameter (5.91 ± 0.16) μm, density 1089 (kg m^{-3}), COMPEL, Bangs Laboratories, Inc.). The curve was measured with a Quantum Design MPMS XL-7 SQUID magnetometer at room temperature (300 K). (a) Magnetic response of the beads in applied magnetic fields ranging from −1 to 1 T; the magnetization of the beads saturates at 4.13 (A m^2 kg^{-1}). (b) View of the magnetization curve for fields ranging from −3.5 to 3.5 mT; remnant magnetization is M_r = 0.28 (A m^2 kg^{-1}). The magnetic susceptibility of the beads χ_{bead} = (0.33 ± 0.06) is calculated from the slope of a line fitted to the initial (*i*) part of the magnetization curve (0–2.5 mT); the spread represents the 95% confidence interval.

Conclusion

This paper modifies the conventional expression for the magnetic force experienced by a superparamagnetic bead to account for the non-zero initial magnetization of the bead. We used the conventional and the modified expressions to model the motion of superparamagnetic beads in a microfluidic channel under the influence of a weak (∼mT) magnetic field produced by electric current passing through a coplanar metal wire. By fitting the model based on the modified expression for the force to the experimental data, we infer that the actual parameters describing the magnetic properties of the beads may deviate significantly from the values provided by the manufacturer. To correct this discrepancy, independent measurements of the magnetic response of the beads should be performed on a sample from the same lot as the beads to be used in an experiment. When a magnetometer is not available, however, the simple microfluidic device described in this note could provide the needed parameters.

The conventional expression for the magnetic force is given in the literature without a derivation or a reference to one,[2,13–18] perhaps because it is considered to be a common knowledge. The lack of an appropriate derivation, however, makes it difficult to decide how this formula should be applied. The conventional formula, for example, does not account for the initial magnetization of the beads, which may contribute significantly to the force in weak magnetic fields. The formula also does not account for the shape of the beads—thus, the effective susceptibility of the beads (not the bulk susceptibility of the constituent materials) must be used. The indiscriminate use of the conventional formula may lead to modeling errors that could be easily avoided.

Manipulation of superparamagnetic beads in suspension under the influence of weak magnetic fields produced by microfabricated electromagnets is becoming increasingly popular in lab-on-a-chip applications. The modified expression for the magnetic force given in this note will help scientists with limited background in physics to predict the motion of the beads accurately.

Appendix

We use eqn (9) describing the magnetic field generated by the wire (electromagnet) and the geometry of the problem to find the magnetic force experienced by the superparamagnetic bead given by the conventional eqn (8). Expanded into component form, eqn (8) becomes eqn (18), where $V = \frac{4}{3}\pi R^3$ is the volume of the bead.

$$\vec{F}_m = \frac{V\chi_{bead}}{\mu_0}\left(\vec{B}\cdot\nabla\right)\vec{B} = \frac{V\chi_{bead}}{\mu_0}\begin{pmatrix} B_x\frac{\partial B_x}{\partial x} + B_y\frac{\partial B_x}{\partial y} + B_z\frac{\partial B_x}{\partial z} \\ B_x\frac{\partial B_y}{\partial x} + B_y\frac{\partial B_y}{\partial y} + B_z\frac{\partial B_y}{\partial z} \\ B_x\frac{\partial B_z}{\partial x} + B_y\frac{\partial B_z}{\partial y} + B_z\frac{\partial B_z}{\partial z} \end{pmatrix} \quad (18)$$

To find the magnetic force (eqn (18)), we need to know the components of the magnetic field $\vec{B}$ vector as well as the various partial derivatives of the magnetic field, which appear in eqn (18).

Calculation of the partial derivatives

In the XY plane $r = x$, and the magnetic field $\vec{B}$ in the geometrical configuration defined in Fig. 3 is given by eqn (19).

$$\vec{B} = \begin{pmatrix} 0 \\ 0 \\ -\frac{\mu_0 I}{2\pi x} \end{pmatrix} \quad i.e. \quad \left\{ B_x = 0, \quad B_y = 0, \quad B_z = -\frac{\mu_0 I}{2\pi x} \right\} \quad (19)$$

Because we assumed that the wire representing the electromagnet is infinitely long along the Y axis, the partial derivatives $\frac{\partial}{\partial y}$ of the components of the vector $\vec{B}$ vanish (eqn (20)).

$$\frac{\partial \vec{B}}{\partial y} = \vec{0} \quad \Rightarrow \quad \left\{ \frac{\partial B_x}{\partial y} = 0, \quad \frac{\partial B_y}{\partial y} = 0, \quad \frac{\partial B_z}{\partial y} = 0 \right\} \quad (20)$$

Because of the symmetry of the system, the partial derivatives of the Y component of $\vec{B}$ along the X and Z axes vanish as well (eqn (21)).

$$\left\{\frac{\partial B_y}{\partial x}=0,\quad \frac{\partial B_y}{\partial z}=0\right\} \tag{21}$$

To find the partial derivatives $\frac{\partial}{\partial z}$ of the components of the vector $\vec{B}$, let us imagine that the bead has shifted along the Z axis from z_0 to z_1 (note that $z_0 > z_1$), while the X and Y coordinates of the bead remained fixed (Fig. 6). The magnetic field vector at the original position of the bead $\vec{B}_0$ is defined by eqn (19) with $x = x_0$ (eqn (22)).

$$\vec{B}_0=\begin{pmatrix}B_{0x}\\B_{0y}\\B_{0z}\end{pmatrix}=\begin{pmatrix}0\\0\\-\frac{\mu_0 I}{2\pi x_0}\end{pmatrix}=\begin{pmatrix}0\\0\\-|\vec{B}_0|\end{pmatrix} \tag{22}$$

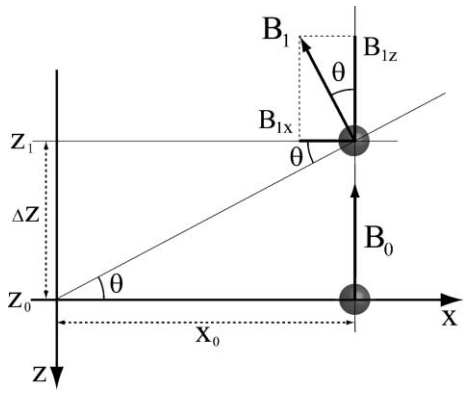

Fig. 6 A schematic illustration of the virtual experiment used to find partial derivatives $\frac{\partial}{\partial z}$ of the applied magnetic field vector $\vec{B}$. In this experiment, we imagine that the superparamagnetic bead has shifted along the Z axis, while the X and Y coordinates of the bead remain fixed (the Y axis is pointing at the reader out of the plane of the page and is not shown). The magnetic field vector at the final position (x_0, z_1) of the bead $\vec{B}(x_0,z_1)\equiv\vec{B}_1=(B_{1x},B_{1z})$ is tilted by an angle of θ radian relative to the direction of the magnetic field vector in the original position of the bead $\vec{B}(x_0,z_0)\equiv\vec{B}_0$. Note that $z_0 > z_1$ and that $\vec{B}_0$ is anti-parallel to the Z axis.

Using the symmetry of the problem, and the basic geometric considerations depicted in Fig. 6, we find the following expression for the components of magnetic field vector at the new position of the bead $\vec{B}_1$ shown in eqn (23).

$$\vec{B}_1=\begin{pmatrix}B_{1x}\\B_{1y}\\B_{1z}\end{pmatrix}=\begin{pmatrix}-|\vec{B}_1|\sin(\theta)\\0\\-|\vec{B}_1|\cos(\theta)\end{pmatrix} \tag{23}$$

By expanding the trigonometric functions into corresponding Taylor series (eqn (24)) and by neglecting small values due to third or higher-order terms for $\Delta z = z_0 - z_1$ and θ, we can re-write eqn (23) as eqn (25).

$$\begin{aligned}\cos(\theta)&=1-\frac{1}{2}\theta^2+\frac{1}{4!}\theta^4+\ldots\\ \sin(\theta)&=\theta-\frac{1}{3!}\theta^3+\ldots\\ \theta&=\arctan\left(\frac{\Delta z}{x_0}\right)=\frac{\Delta z}{x_0}-\frac{1}{3}\left(\frac{\Delta z}{x_0}\right)^3+\ldots\end{aligned} \tag{24}$$

$$\begin{aligned}B_{1x}&=-|\vec{B}_1|\sin(\theta)=-|\vec{B}_1|\theta=-|\vec{B}_1|\frac{\Delta z}{x_0}\\ B_{1z}&=-|\vec{B}_1|\cos(\theta)=-|\vec{B}_1|\left(1-\frac{1}{2}\theta^2\right)=\\ &-|\vec{B}_1|\left(1-\frac{1}{2}\left(\frac{\Delta z}{x_0}\right)^2\right)\end{aligned} \tag{25}$$

To find the magnitude of the magnetic field at the new position of the bead $|\vec{B}_1|$, we substitute $r=x_0\left(1+(\Delta z/x_0)^2\right)^{\frac{1}{2}}$ into eqn (9) and apply the Taylor series expansion to obtain eqn (26), where $|\vec{B}_0|=\frac{\mu_0 I}{2\pi x_0}$ is the magnitude of magnetic field at the original position of the bead $\vec{B}_0$ (Fig. 6).

$$\begin{aligned}|\vec{B}_1|&=\frac{\mu_0 I}{2\pi r}=\frac{\mu_0 I}{2\pi x_0}\left(1+(\Delta z/x_0)^2\right)^{-\frac{1}{2}}\\ &=|\vec{B}_0|\left(1-\frac{1}{2}\left(\frac{\Delta z}{x_0}\right)^2+\frac{3}{8}\left(\frac{\Delta z}{x_0}\right)^4+\ldots\right)\end{aligned} \tag{26}$$

We use eqn (26) and neglect third and higher-order terms for Δz to express the X and Z components of the vector $\vec{B}_1$ (eqn (25)) through the magnitude of the field at the original position of the bead $|\vec{B}_0|$ and obtain eqn (27).

$$\begin{aligned}B_{1x}&=-|\vec{B}_1|\frac{\Delta z}{x_0}=-|\vec{B}_0|\left(1-\frac{1}{2}\left(\frac{\Delta z}{x_0}\right)^2\right)\frac{\Delta z}{x_0}=-\frac{|\vec{B}_0|}{x_0}\Delta z\\ B_{1z}&=-|\vec{B}_1|\left(1-\frac{1}{2}\left(\frac{\Delta z}{x_0}\right)^2\right)=\\ &-|\vec{B}_0|\left(1-\frac{1}{2}\left(\frac{\Delta z}{x_0}\right)^2\right)\left(1-\frac{1}{2}\left(\frac{\Delta z}{x_0}\right)^2\right)=-|\vec{B}_0|+|\vec{B}_0|\left(\frac{\Delta z}{x_0}\right)^2\end{aligned} \tag{27}$$

We can now compute the partial derivatives $\frac{\partial}{\partial z}$ of the components of the vector $\vec{B}$ as shown in eqn (28).

$$\begin{aligned}&\frac{\partial B_z}{\partial z}\equiv\lim_{z_1\to z_0}\frac{B_z(z_1)-B_z(z_0)}{z_1-z_0}=\lim_{z_1\to z_0}\frac{B_{1z}-B_{0z}}{z_1-z_0}=\\ &\lim_{z_1\to z_0}\frac{-|\vec{B}_0|+|\vec{B}_0|\left(\frac{\Delta z}{x_0}\right)^2+|\vec{B}_0|}{z_1-z_0}=\\ &=\lim_{z_1\to z_0}\frac{|\vec{B}_0|\left(\frac{z_0-z_1}{x_0}\right)^2}{z_1-z_0}=\lim_{z_1\to z_0}\frac{|\vec{B}_0|\left(\frac{z_1-z_0}{x_0}\right)^2}{z_1-z_0}=\\ &\lim_{z_1\to z_0}\left(\frac{|\vec{B}_0|}{x_0^2}(z_1-z_0)\right)=0\\ &\frac{\partial B_x}{\partial z}\equiv\lim_{z_1\to z_0}\frac{B_x(z_1)-B_x(z_0)}{z_1-z_0}=\lim_{z_1\to z_0}\frac{B_{1x}-B_{0x}}{z_1-z_0}=\\ &\lim_{z_1\to z_0}\frac{-\frac{|\vec{B}_0|}{x_0}\Delta z-0}{z_1-z_0}=\lim_{z_1\to z_0}\frac{-\frac{|\vec{B}_0|}{x_0}(z_0-z_1)}{z_1-z_0}=\\ &=\lim_{z_1\to z_0}\frac{\frac{|\vec{B}_0|}{x_0}(z_1-z_0)}{z_1-z_0}=\lim_{z_1\to z_0}\left(\frac{|\vec{B}_0|}{x_0}\right)=\frac{\mu_0 I}{2\pi x_0^2},\forall x_0\end{aligned} \tag{28}$$

Because eqn (28) is true for any x_0, we finally find the partial derivatives (eqn (29)).

$$\left\{\frac{\partial B_x}{\partial z}=\frac{\mu_0 \mathrm{I}}{2\pi x^2},\quad \frac{\partial B_z}{\partial z}=0\right\} \tag{29}$$

Computation of the force

After the substitution of eqn (19), (21) and (29) into eqn (18), the conventional expression for the force becomes eqn (30).

$$\vec{F}_\mathrm{m}=\begin{pmatrix} -\dfrac{\chi_\mathrm{bead} R^3 \mu_0 \mathrm{I}^2}{3\pi x^3} \\ 0 \\ 0 \end{pmatrix} \tag{30}$$

The modified expression for the magnetic force given by eqn (7), when expanded into the component form, becomes eqn (31).

$$\vec{F}_\mathrm{m}=\rho V\begin{pmatrix} M_{0x}\dfrac{\partial B_x}{\partial x}+M_{0y}\dfrac{\partial B_x}{\partial y}+M_{0z}\dfrac{\partial B_x}{\partial z} \\ M_{0x}\dfrac{\partial B_y}{\partial x}+M_{0y}\dfrac{\partial B_y}{\partial y}+M_{0z}\dfrac{\partial B_y}{\partial z} \\ M_{0x}\dfrac{\partial B_z}{\partial x}+M_{0y}\dfrac{\partial B_z}{\partial y}+M_{0z}\dfrac{\partial B_z}{\partial z} \end{pmatrix}+ \frac{V\chi_\mathrm{bead}}{\mu_0}\begin{pmatrix} B_x\dfrac{\partial B_x}{\partial x}+B_y\dfrac{\partial B_x}{\partial y}+B_z\dfrac{\partial B_x}{\partial z} \\ B_x\dfrac{\partial B_y}{\partial x}+B_y\dfrac{\partial B_y}{\partial y}+B_z\dfrac{\partial B_y}{\partial z} \\ B_x\dfrac{\partial B_z}{\partial x}+B_y\dfrac{\partial B_z}{\partial y}+B_z\dfrac{\partial B_z}{\partial z} \end{pmatrix} \tag{31}$$

To evaluate eqn (31) we need to know the components of the initial magnetization $\vec{M}_0$. Because the bead can rotate freely in suspension, the initial magnetization of the bead $\vec{M}_0$ is parallel to the applied magnetic field $\vec{B}$ (eq 32) (note that $\vec{M}_0$ is *anti-parallel* to the Z axis (Fig. 3)).

$$\vec{M}_0=\begin{pmatrix} 0 \\ 0 \\ -M_0 \end{pmatrix} \textit{ i.e. } \left\{M_{0x}=0,\quad M_{0y}=0,\quad M_{0z}=-M_0\right\} \tag{32}$$

By substituting eqn (19), (21), (29), and (32) into eqn (31), we obtain the following expression for the force (eqn (33)).

$$\vec{F}_\mathrm{m}=\begin{pmatrix} -\dfrac{2\rho M_0 R^3 \mu_0 \mathrm{I}}{3x^2}-\dfrac{\chi_\mathrm{bead} R^3 \mu_0 \mathrm{I}^2}{3\pi x^3} \\ 0 \\ 0 \end{pmatrix} \tag{33}$$

We see from eqns (30) and (33) that the only component of the magnetic force vector that is not zero is the X component. This means that a superparamagnetic bead positioned in the XY plane would experience a force in the direction along the X axis towards the Y axis. This answer is intuitive—one would expect a superparamagnetic bead to move towards a magnet.

Acknowledgements

This research was supported by the National Institutes of Health (NIH) (GM065364). This work was performed in part at the Center for Nanoscale Systems (CNS), a member of the National Nanotechnology Infrastructure Network (NNIN), which is supported by the National Science Foundation under NSF award no. ECS-0335765. CNS is part of the Faculty of Arts and Sciences at Harvard University. This work made use of the MRSEC Shared Experimental Facilities at MIT, supported by the National Science Foundation under award number DMR-02-13282. We thank Dr Shaoyan Chu of the Crystal Growth shared experimental facility in the Center for Materials Science and Engineering (CMSE) at MIT for his help with the SQUID magnetometer. A.C.S. gratefully acknowledges a predoctoral fellowship from the Howard Hughes Medical Institute.

References

1 I. Safarik and M. Safarikova, *J. Chromatogr., B: Biomed. Appl.*, 1999, **722**, 33–53.
2 N. Pamme, *Lab Chip*, 2006, **6**, 24–38.
3 M. A. M. Gijs, *Microfluid. Nanofluid.*, 2004, **1**, 22–40.
4 A. Ito, M. Shinkai, H. Honda and T. Kobayashi, *J. Biosci. Bioeng.*, 2005, **100**, 1–11.
5 H. Lee, A. M. Purdon and R. M. Westervelt, *Appl. Phys. Lett.*, 2004, **85**, 1063–1065.
6 V. I. Furdui, J. K. Kariuki and D. J. Harrison, *J. Micromech. Microeng.*, 2003, **13**, S164–S170.
7 D. W. Inglis, R. Riehn, R. H. Austin and J. C. Sturm, *Appl. Phys. Lett.*, 2004, **85**, 5093–5095.
8 N. Xia, T. P. Hunt, B. T. Mayers, E. Alsberg, G. M. Whitesides, R. M. Westervelt and D. E. Ingber, *Biomed. Microdev.*, 2006, **8**, 299–308.
9 D. Islam and A. A. Lindberg, *J. Clin. Microbiol.*, 1992, **30**, 2801–2806.
10 J. W. Choi, K. W. Oh, J. H. Thomas, W. R. Heineman, H. B. Halsall, J. H. Nevin, A. J. Helmicki, H. T. Henderson and C. H. Ahn, *Lab Chip*, 2002, **2**, 27–30.
11 N. Wang, J. P. Butler and D. E. Ingber, *Science*, 1993, **260**, 1124–1127.
12 A. C. Siegel, S. S. Shevkoplyas, D. B. Weibel, D. A. Bruzewicz, A. W. Martinez and G. M. Whitesides, *Angew. Chem., Int. Ed.*, 2006, **45**, 6877–6882.
13 J. J. Chalmers, Y. Zhao, M. Nakamura, K. Melnik, L. Lasky, L. Moore and M. Zborowski, *J. Magn. Magn. Mater.*, 1999, **194**, 231–241.
14 M. Grumann, A. Geipel, L. Riegger, R. Zengerle and J. Ducree, *Lab Chip*, 2005, **5**, 560–565.
15 K. H. Han and A. B. Frazier, *J. Appl. Phys.*, 2004, **96**, 5797–5802.
16 N. Pekas, M. Granger, M. Tondra, A. Popple and M. D. Porter, *J. Magn. Magn. Mater.*, 2005, **293**, 584–588.
17 H. Suzuki, C. M. Ho and N. Kasagi, *J. Microelectromech. Syst.*, 2004, **13**, 779–790.
18 M. Tondra, M. Granger, R. Fuerst, M. Porter, C. Nordman, J. Taylor and S. Akou, *IEEE Trans. Magn.*, 2001, **37**, 2621–2623.
19 BioMag, Bangs Laboratories, Inc., www.bangslabs.com/products/bangs/biomag_products.php.
20 COMPEL, Bangs Laboratories, Inc., www.bangslabs.com/technotes/102.pdf.
21 MicroParticles, MicroParticles GmbH, www.microparticles.de/superparamagnetic_particles.html.
22 SPHERO, Spherotech, Inc., www.spherotech.com/para_par.htm.
23 K. van Ommering, J. H. Nieuwenhuis, L. J. van Ijzendoorn, B. Koopmans and M. W. J. Prins, *Appl. Phys. Lett.*, 2006, **89**, 142511.
24 R. C. Black and F. C. Wellstood, in *The SQUID Handbook: Applications of SQUIDs and SQUID Systems*, ed. J. Clarke and

A. I. Braginski, WILEY-VCH Verlag GmbH & Co. KGaA, Weinheim, Germany, 2006, vol. 2.
25 MPMS Application Note 1014–208 A, Quantum Design, Inc., 2001.
26 Most SQUID magnetometers do not feature a sensor of the applied magnetic field—the field is set by adjusting the persistent current in the superconducting magnet of the magnetometer. When the magnet is discharged from very high (>1 T) or very low (<−1 T) magnetic fields to zero in the no overshoot mode (in which the field is approached monotonically from one direction without overshooting the target value), the superconducting wires of the magnet trap magnetic flux—the resulting remnant field can be as high as ±3 mT. At low fields (<10 mT), the remnant field is equivalent to a constant field superimposed on the field produced by the persistent current in the magnet of the magnetometer.
27 *CRC Handbook of Chemistry and Physics, Internet Version 2006*, ed. D. R. Lide, Taylor and Francis, Boca Raton, FL, USA, 2006.
28 A. Winkleman, K. L. Gudiksen, D. Ryan, G. M. Whitesides, D. Greenfield and M. Prentiss, *Appl. Phys. Lett.*, 2004, **85**, 2411–2413.
29 The discussion of highly concentrated solutions of paramagnetic ions and ferrofluids as the suspending media is beyond the scope of this paper.
30 J. D. Jackson, *Classical Electrodynamics.*, John Wiley and Sons, Inc., Hoboken, NJ, USA, 3rd edn, 1999.
31 E. M. Purcell, *Electricity and Magnetism*, McGraw-Hill, Inc., New York, NY, USA, 2nd edn, 1985.
32 B. I. Bleaney and B. Bleaney, *Electricity and Magnetism*, Oxford University Press, Oxford, England, New York, USA, 3rd edn, 1989.
33 R. Serway, R. Beichner and J. Jewett, *Physics for Scientists and Engineers*, Thomson Learning, Inc., 5th edn, 2000.
34 G. K. Batchelor, *An Introduction to Fluid Dynamics*, Cambridge University Press, Cambridge, England, 2000.

